

**UNIVERSIDAD SAN FRANCISCO DE QUITO USFQ**

**Colegio de Ciencias e Ingenierías**

**Optical trapping of metal nanoshells embedding gain  
molecules**

**Proyecto de investigación**

**Jonathan Joel Sánchez Jácome**

**Licenciatura en Física**

Trabajo de titulación presentado como requisito  
para la obtención del título de Licenciado en Física

Quito, 15 de mayo de 2019

UNIVERSIDAD SAN FRANCISCO DE QUITO USFQ  
COLEGIO DE CIENCIAS E INGENIERÍAS

**HOJA DE CALIFICACIÓN  
DE TRABAJO DE TITULACIÓN**

**Optical trapping of metal nanoshells embedding gain molecules**

**Jonathan Joel Sánchez Jácome**

Calificación:

Nombre del profesor: Melissa Infusino Ph.D.

Firma del profesor: \_\_\_\_\_

Quito, 15 de mayo de 2019

## DERECHOS DE AUTOR

Por medio del presente documento certifico que he leído todas las Políticas y Manuales de la Universidad San Francisco de Quito USFQ, incluyendo la Política de Propiedad Intelectual USFQ, y estoy de acuerdo con su contenido, por lo que los derechos de propiedad intelectual del presente trabajo quedan sujetos a lo dispuesto en esas Políticas.

Asimismo, autorizo a la USFQ para que realice la digitalización y publicación de este trabajo en el repositorio virtual, de conformidad a lo dispuesto en el Art. 144 de la Ley Orgánica de Educación Superior.

Firma del estudiante: -----

Nombres y apellidos: Jonathan Joel Sánchez Jácome

Código: 00118005

Cédula de identidad: 172396519-8

Lugar y fecha: Quito, 15 de mayo de 2019

*A mis padres.*

## ***Agradecimientos***

*Agradezco a todos mis profesores por el conocimiento que me han legado, en especial a Melissa por la paciencia y dedicación que le empeño a este proyecto de titulación. A mis compañeros y amigos por las inolvidables experiencias durante estos años. Y a mis padres por ser el apoyo durante mi proyecto de vida.*

## Resumen

En este proyecto de tesis se estudiaron las pinzas ópticas en una nanoshell metálico con moléculas incrustadas en la aproximación dipolar. En estas el fenómeno de la energía transmitida entre las moléculas de ganancia y los plasmones de superficie resonantes afecta la polarizabilidad de la partícula, y por ende cambian la fuerzas ópticas de atrapamiento. La polarizabilidad fue calculada numericamente para 6 niveles de ganancia en el regimen quasistático (0, -0.044, -0.088, -0.132, -0.176, -0.22). La fuerzas ópticas se calcularon en estos 6 niveles de ganancia para dos tipos arreglos: Rayos Gaussianos contrapopagantes, y un solo rayo Gaussiano. Finalmente, las fuerzas se aproximaron como lineales alrededor de la posición de equilibrio demostrando que la eficiencia de la trampa aumenta significativamente con el nivel de ganancia.

**Key words:** Pinzas ópticas, optica geométrica, aproximacion de dipolo, quasistatico, nanoshell, resonancia plasmonica, moléculas fluorecentes, rayo Gaussiano.

## Abstract

In this thesis project OT were studied with trapped metallic nanoshells embedding gain molecules by using the dipole approximation. Here the phenomenon of the resonant energy transfer between gain molecules and the surface plasmon resonance affect the particle polarizability thus changing the optical forces generated in the trap. The polarizability was numerically calculated for six gain levels in the steady-state regime (0, -0.044, -0.088, -0.132, -0.176, -0.22). Optical forces were calculated for the 6 gain levels in two arrangements: counter propagating Gaussian beams and a single Gaussian beam. Finally, the forces were approximated as linear around the equilibrium position demonstrating that the efficiency of the trap significantly increases with the gain levels.

**Key words:** Optical tweezers, geometrical optics, dipole approximation, steady-state, nanoshell, plasmonic resonance, dye molecules, Gaussian beam.

# Index

<b>1</b>	<b>Introduction</b>	<b>9</b>
1.1	OT in the Geometrical Optics regime . . . . .	9
1.2	OT in the Dipole approximation . . . . .	12
1.2.1	Calculation of the optical forces . . . . .	12
<b>2</b>	<b>Metallic nanoshell with gain</b>	<b>15</b>
2.1	Polarizability in a nanoshell . . . . .	15
2.2	Polarization of a metallic nanoshell with gain material . . . . .	17
<b>3</b>	<b>Results and discussion</b>	<b>20</b>
3.1	OT counterpropagating Beams . . . . .	23
3.2	OT single Gaussian beam . . . . .	27
<b>4</b>	<b>Conclusions</b>	<b>32</b>
<b>5</b>	<b>References</b>	<b>33</b>

# 1 Introduction

Optical tweezers (OTs) are a well-known tool for manipulation of micro and nanoparticles. They were demonstrated for the first time in 1970 by Arthur Ashkin [1]. Essentially, an OT is a device that allows to capture and move objects in a wide range of sizes, from atoms to microsized beads by using tightly focused laser beams. In these devices, the trapping is produced by the transmission of momentum between the laser and the particle [2]. OT experiments allow to measure with high precision the forces acting on the trapped particle even if they are very small, typically of the order piconewtons.

## 1.1 OT in the Geometrical Optics regime

Optical tweezers (OTs) are a device that traps particles by using lasers. If the size of the particle is much larger than the wavelength  $\lambda \ll a$ , it is possible to analyze these phenomena in the geometrical optics regime, that means that the laser can be considered as a ray and its interaction with matter can be reduced to the Snell's law for diffraction [2] (See: Figure 1). The ray impinging on the particle is partially reflected and partially transmitted: this corresponds to a change in the light momentum that due to Newton's action-reaction law results in a force acting on the particle (See Equation 1 where  $N$  is the number of photons,  $p$  is the momentum per photon,  $P$  is the light power). This mechanism is known as radiation pressure and it is also observed in the comet tails where the stream of dust is caused by the sun-light pushing it away [2].

$$\vec{F}_{reflection} = -2Np\hat{u} = -\frac{2P}{c}\hat{u} \quad (1)$$

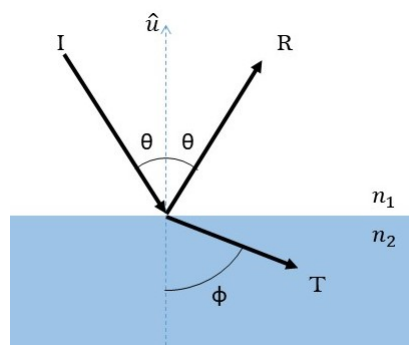


Figure 1: Snell law for diffraction. In the interface the incident Ray (I) is partially reflected (R) and partially transmitted (T). The angle  $\theta$  formed between I and R is equal. The angle  $\phi$  depends on the refraction indexes. If  $n_1 > n_2$  then  $\theta < \phi$ . If  $n_1 < n_2$  then  $\theta > \phi$ .

If a ray impinges a spherical particle such that the absorption losses are negligible, then the transmitted ray will be refracted many times as shown in Figure 2. The resulting force on the particle is the sum of the contributions generated in each of those multiple refraction events. For comfort and convention, the net force can be separated into parallel and perpendicular components (to the propagation direction), each one known as scattering and gradient force respectively (Equation 2).

$$\vec{F}_{ray} = F_{sct}\hat{r}_{\parallel} + F_{grad}\hat{r}_{\perp} \quad (2)$$

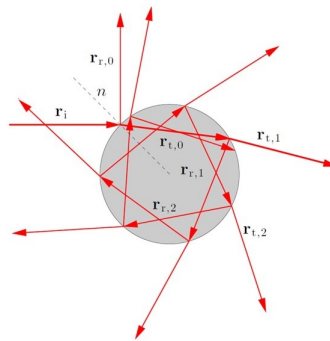


Figure 2: Particle Under multiple refraction events.  $r_i$  is the incident ray on the spherical surface with normal  $n$ .  $r_{r,j}$  is the  $j$  reflected ray.  $r_{t,j}$  is the  $j$  transmitted ray[2].

The sign of the gradient force depends on the relation between the indexes of refraction of the particle and the surrounding medium, being negative (trapping) if the index of refraction of the particle is larger than the one of the surrounding medium or positive in the opposite case (particle is pushed away)Figure 3.a;b. Anyway the scattering force always pushes the particle in the parallel direction, preventing the possibility of an effective trapping. There are two options to achieve optical trapping. The first method consist in using two counter propagating laser beams so that the scattering forces are opposite and cancel each other[2]. The method still works if there is an angle between the rays, but only if the angle is big enough otherwise the scattering force will prevail.(See Figure 3.d;c).

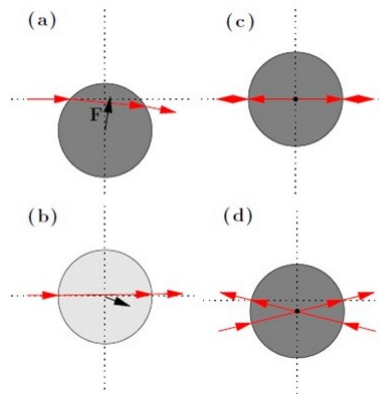


Figure 3: a) A Glass sphere ( $n_g$ ) immersed in water( $n_m$ ) and illuminated by a single ray is attracted toward the propagation axis by the gradient force since  $n_g > n_m$ , but it is also pushed in the propagation direction by the scattering force. b) An Air sphere ( $n_a$ ) immersed in water( $n_m$ ) and illuminated by a ray is pushed away from the propagation axis since  $n_a < n_m$ . c) The addition of a second counter-propagating ray produces an effective trapping d) Two counter-propagating rays at an angle can generate a stable trapping ( $n_g$ )[2].

There is a more popular method, commonly referred in literature as optical tweezers, that allows to achieve the trapping by using a highly-focused single beam[2]. The technique is based on the use of an objective microscope with a high numerical aperture (NA) that allows to trap and image the particle at the same time. The beam can be decomposed in a pack of parallel rays that converges to the focal point when focused by the objective-lens. Each ray interacts with the sphere and will contribute to the net force. If the NA is big enough the most external rays will work similarly to two counter-propagating rays at an angle. This implies that trapping in the parallel direction depends strongly on the NA as shown in Figure4.

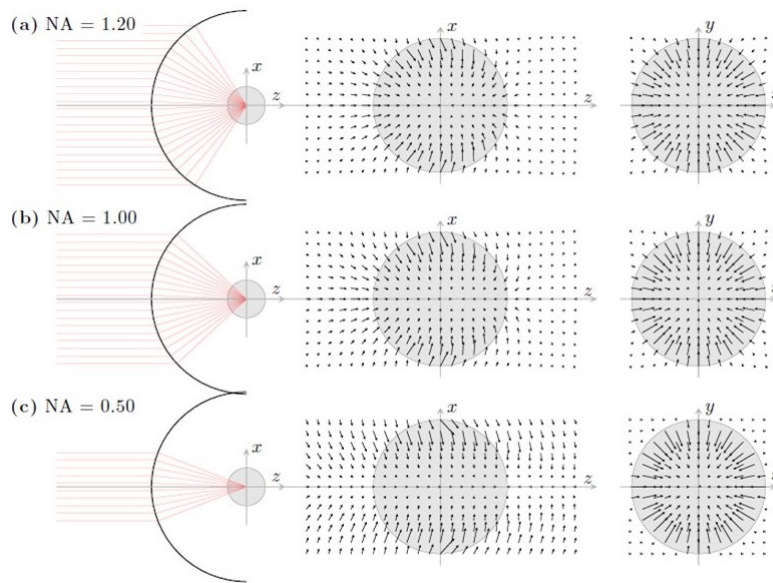


Figure 4: Optical Forces in the longitudinal ( $xz$ ) and transverse plane ( $xy$ ) as a function of NA produced by a focused beam on a glass ( $n_g$ ) sphere immersed in water ( $n_m$ ). As NA decreases, the parallel trapping is lost due to the scattering forces[?].

## 1.2 OT in the Dipole approximation

The geometrical optics regime is very useful to explain the working principle of optical trapping and we introduced it for sake of clearness and completeness. However in our project we are dealing with the trapping of nano-objects, so geometrical optics approximation does not apply. When the wavelength is way bigger than the size of the particle  $a \ll \lambda$ , the picture of the OTs is quite different and we can calculate optical forces by using dipole approximation. Particle-light interaction can be described as an oscillating dipole excited by an electromagnetic wave[2].

As we will see in the next sections the optical forces depends on the polarizability of the particle  $\alpha$ , defined in Equation 3, where  $\vec{p}$  is the particle dipole momentum and  $\vec{e}$  is the external electric field.

$$\vec{p} = \alpha \vec{e} \quad (3)$$

### 1.2.1 Calculation of the optical forces

Previously in this subsection we will calculate the force acting on a dipole in the presence of a homogeneous time-varying electromagnetic field. We consider a dipole with mass  $m$  and charges  $\pm q$ , with positions  $\vec{r}_\pm$  respectively, and separated away by

$\Delta\vec{r} = \vec{r}_+ - \vec{r}_-$ . The equations of motion for these charges are governed by the Lorentz forces and by the force arising from Coulomb interaction  $U_{int}$ :

$$m^2 \frac{d^2 \vec{r}_\pm}{dt^2} = \pm [\vec{\varepsilon}_i(\vec{r}_\pm, t) + \frac{d\vec{r}_\pm}{dt} \times \vec{B}_i(\vec{r}_\pm, t)] \mp \vec{\nabla} U_{int}(\Delta\vec{r}, t) \quad (4)$$

Consider now the position of the center of mass  $\vec{r}_d$  (Equation 5)

$$\vec{r}_d = \frac{\vec{r}_+ + \vec{r}_-}{2} \quad (5)$$

By using the approximation  $|\vec{r}_\pm - \vec{r}_d| \ll |\vec{r}_d|$  it is possible to expand  $\vec{\varepsilon}_i(\vec{r}_\pm, t)$  and  $\vec{B}_i(\vec{r}_\pm, t)$  in Taylor series around the center of mass of the dipole:

$$\begin{aligned} \vec{\varepsilon}_i(\vec{r}_\pm, t) &= \vec{\varepsilon}_i(\vec{r}_d, t) + ((\vec{r}_\pm - \vec{r}_d) \cdot \vec{\nabla}) \vec{\varepsilon}_i(\vec{r}_d, t) \\ \vec{B}_i(\vec{r}_\pm, t) &= \vec{B}_i(\vec{r}_d, t) + ((\vec{r}_\pm - \vec{r}_d) \cdot \vec{\nabla}) \vec{B}_i(\vec{r}_d, t) \end{aligned} \quad (6)$$

Substituting these expressions and summing up the two equations in (4) we obtain:

$$\vec{F}_d(\vec{r}_d, t) = (\vec{p}_d \cdot \vec{\nabla}) \vec{\varepsilon}_i(\vec{r}_d, t) + \vec{p}_d \times (\vec{\nabla} \times \vec{\varepsilon}_i(\vec{r}_d, t)) + \frac{d}{dt} (\vec{p}_d \times \vec{B}_i(\vec{r}_d, t)), \quad (7)$$

where  $\vec{p}_d = q(\vec{r}_+ - \vec{r}_-)$  is the dipole momentum. A the complete deduction of this equation can be found in the bibliography [2].

This is a varying in time force. In order to obtains an effective force its necessary to average 7 in a period of oscillation of the fields  $T = \frac{2\pi}{\omega}$ . The last term vanish and give us an equation that can be written in terms of the electric field phasor, the polarizability and the extinction cross section (the complete deduction can be found in [2]):

$$\vec{F}_d = \frac{1}{4} \alpha' \vec{\nabla} |\vec{E}_i|^2 + \frac{\sigma_{ext}}{c} \vec{S}_i - \frac{1}{2} \sigma_{ext} c \vec{\nabla} \times \vec{s}_d \quad (8)$$

Equation 8 presents three terms, each one describes a different force.

The first term is known as the ‘‘gradient’’ force and it is extremely important since is the one responsible for the optical trapping, it is related to the gradient of the intensity and the real part of the polarizability (9).

$$\vec{F}_{gradient}(\rho) = \frac{1}{2} \frac{\alpha'}{c \epsilon_0} \vec{\nabla}_\rho I \approx -k_\rho \rho \hat{r}_\rho \quad (9)$$

It means that if a particle has a positive polarizability ( $\alpha'$ ) it will be always attracted toward regions of higher intensity. A tightly focused Gaussian beam will indeed be able to trap this kind of particles in its beam waist, while it will push away particles with negative polarizability. For this reason the gradient force is regarded as a restoring force and a spring-like constant  $k_\rho$  can be defined, as soon as the particle is displaced

of  $\rho$  from the equilibrium position in an arbitrary direction the gradient force will push it back. The elastic constant of an optical trap is one the most important parameters it is known as trap stiffness and it tell us if the trap will be able to overcome thermal agitations.

In case of a Gaussian beam, like in our calculation, the value of the constant  $k_\rho$  in the perpendicular direction is given by:

$$k_\rho = 2 \frac{\alpha'}{c\epsilon_0} \frac{I_0}{\omega_0^2} \quad (10)$$

We can notice that the constant depends on the light intensity, on the particle polarizability and to the size of the beam ( $\omega_0$  is the beam waist), that means that the tighter focusing corresponds to stronger traps (Figure 5).

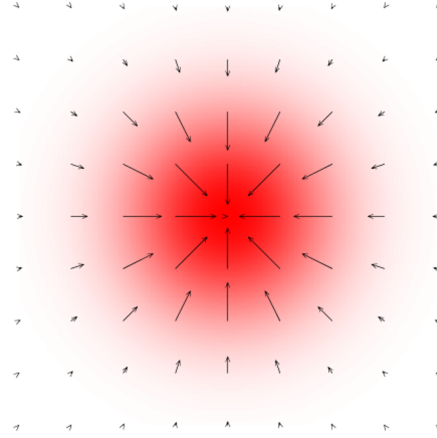


Figure 5: In red, intensity distribution in the plane perpendicular to the propagation. Black arrows represent the gradient forces acting on a particle with positive polarizability in the plane perpendicular to the propagation. [2]

The second term is known as scattering force. It is parallel to the pointing vector  $\vec{S}$ , and can be expressed in terms of the extinction cross section, since it is originated from the scattering and absorption of light by the particle. This is detrimental, because in order to have a stable trapping the axial component of the gradient force must overcome the scattering force.

$$\vec{F}_{scattering}(\vec{r}) = \frac{n_m}{c} \sigma_{ext} I(\vec{r}) \hat{r}_{\parallel} \quad (11)$$

The final term is the spin-curl force that is different from zero only when the polarization of the trapping beam is not uniform. Since in our calculation we are assuming the trapping beam has linear and uniform polarization, this term is not taken into account.

## 2 Metallic nanoshell with gain

In the previous section we described how it is possible to calculate the optical forces in a dipole approximation just by knowing the polarizability. This project is addressed to the study of OT applied to gain-functionalized metallic nanoshells (NS). The reason for which we have chosen metallic-nanoshell is that they support localized surface plasmon resonance (LSP). LSPR is an excitation of the conduction electrons of metallic nanostructures coupled to an electromagnetic field"[3]. It is an extremely interesting phenomenon since it allows to concentrate very intense electric field at the nanoscale, for these reason nanoshell are a promising candidate for cancer therapies based on nanomedicine[4]. In our project we are interested in the coupling between LSPR and the emission of an externally pumped active medium inside the nanoshell. This coupling has been object of extensive studies in last years since it is a possible strategy for the compensation of metallic losses, present at the resonance frequency[5, 6]. Since the coupling is strongly affecting the nano-shell polarizability, and since the polarizability determine the optical forces we decided to calculate the optical forces for a nanoshell embedding dye molecules, for different levels of gain. Experimentally the gain level can be changed by changing the laser pump power. The nanoparticles object of our study are characterized by a dielectric core made of silica embedding dye molecules, surrounded by a thin silver shell. In our calculation we considered nano-shell with a overall radius of 20 nm, with different dimension of the metallic shell. It is known that in metallic nanoshell the optical resonance is extraordinarily sensitive to the inner and outer dimensions of the metallic shell layer[7].

### 2.1 Polarizability in a nanoshell

In the previous section we described how it is possible to calculate the optical forces in a dipole approximation just by knowing the polarizability.

In the previous section approach to understand the polarizability in a NS is the more simplistic nanoparticle. Lets consider an ideal core shell particle with internal radius  $a_1$  and external radius  $a_2$  immersed in an external field  $\vec{E}_i = E_i \hat{k}$ . Assuming that the system reaches a quasi static equilibrium just as the previous examples it is possible to calculate the field in each region  $\vec{E}_{1,2,3} = -\vec{\nabla} \Phi_{1,2,3}$  utilizing the Laplace equation.

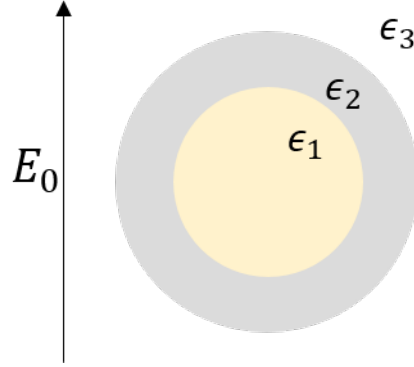


Figure 6: NS structure with (core's and shell's permittivities  $\epsilon_1$  and  $\epsilon_2$  respectively) is surrounded by a medium with permittivity  $\epsilon_3$ . This system is immersed in a uniform electric field  $\vec{E}_0$ .

$$\nabla^2 \Phi_{1,2,3} = 0 \quad (12)$$

Given the symmetry of the system the electric potential in spherical coordinates is

$$\Phi_{1,2,3}(r, \theta) = \sum_{l=0}^{\infty} [\tilde{p}_l^{1,2,3} r^l + \frac{p_l^{1,2,3}}{r^{l+1}}] P_l(\cos\theta) \quad (13)$$

Now its important to consider that the field should always be well defined, so considering the region number 1 its important to notice that the field should not diverge for  $r = 0$  which means that  $p_l^1 = 0$  for any  $l$ . Also for large distances the radiated field fades away and the only remaining should be the external field

$$\lim_{r \rightarrow \infty} \Phi_3(r, \theta) = -E_i r \cos\theta \quad (14)$$

Consequently,  $\tilde{p}_l^3 = 0$  for  $l \neq 1$  and  $\tilde{p}_1^3 = -E_i$ .

then the solutions for each region remains as follows.

$$\Phi_1(r, \theta) = \sum_{l=0}^{\infty} \tilde{p}_l^1 r^l P_l(\cos\theta) \quad (15)$$

$$\Phi_2(r, \theta) = \sum_{l=0}^{\infty} [\tilde{p}_l^2 r^l + \frac{p_l^2}{r^{l+1}}] P_l(\cos\theta) \quad (16)$$

$$\Phi_3(r, \theta) = \sum_{l=0}^{\infty} [-\delta_{l,1} r E_i + \frac{p_l^3}{r^{l+1}}] P_l(\cos\theta) \quad (17)$$

Applying all border conditions the  $p_l^3$  and so the external field as function of the incident field we obtain the complete deduction can be found in the literature[8].

$$p_l^3 = a_2^{l+2} \frac{(\epsilon_1 - \epsilon_2)[l\epsilon_1 + (l+1)\epsilon_2] + \rho^{2l+1}(\epsilon_1 - \epsilon_2)[l\epsilon_2 + (l+1)\epsilon_3]}{[l\epsilon_1 + (l+1)\epsilon_2][l\epsilon_2 + (l+1)\epsilon_3] - l(l+1)\rho^{2l+1}(\epsilon_1 - \epsilon_2)(\epsilon_3 - \epsilon_2)} E_i \delta_{l,1} \quad (18)$$

considering only the dipole approximation  $l = 1$  the formula 18 reduces giving a similar relation that we are familiar with equation 3

$$p^3 = a_2^3 \frac{(\epsilon_1 - \epsilon_2)(\epsilon_1 + 2\epsilon_2) + \rho^3(\epsilon_1 - \epsilon_2)(\epsilon_2 + 2\epsilon_3)}{(\epsilon_1 + 2\epsilon_2)(\epsilon_2 + 2\epsilon_3) - 2\rho^3(\epsilon_1 - \epsilon_2)(\epsilon_3 - \epsilon_2)} E_i \quad (19)$$

where the polarizability is given by Equation 19 that depends purely on the dielectric constants, the external-internal ratio  $\rho = \frac{a_2}{a_1}$ .

$$\alpha = \frac{3V}{4\pi} \frac{(\epsilon_1 - \epsilon_2)(\epsilon_1 + 2\epsilon_2) + \rho^3(\epsilon_1 - \epsilon_2)(\epsilon_2 + 2\epsilon_3)}{[1\epsilon_1 + 2\epsilon_2](\epsilon_2 + 2\epsilon_3) - 2\rho^3(\epsilon_1 - \epsilon_2)(\epsilon_3 - \epsilon_2)} \quad (20)$$

## 2.2 Polarization of a metallic nanoshell with gain material

The calculation of the polarizability is quite different if we consider the presence of gain molecules in the region 1 and a metallic material in the region 2 (figure 7). In order to obtain a new formulation, we may write the field equations in terms of the displacement field  $\vec{D} = \epsilon_0 \vec{E} + \vec{P}$

$$\vec{D}_1 = \epsilon_0 \epsilon_b \vec{E}_1 + 2\vec{\Pi}^* = \epsilon_0 \epsilon_b (-\vec{\nabla} \Phi_1) + 2(-\vec{\nabla} \psi_1)^* \quad (21)$$

$$\vec{D}_2 = \epsilon_0 \vec{E}_2 + \epsilon_0 \chi_m \vec{P}_2 = \epsilon_0 (-\vec{\nabla} \Phi_2) + \epsilon_0 \chi_m (-\vec{\nabla} \psi_2) \quad (22)$$

$$\vec{D}_3 = \epsilon_0 \epsilon_3 \vec{E}_3 = \epsilon_0 \epsilon_3 (-\vec{\nabla} \Phi_3) \quad (23)$$

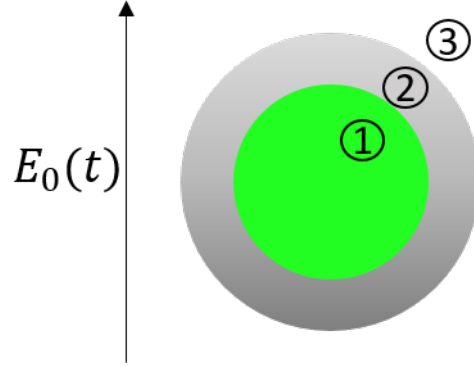


Figure 7: NS with a gaining made core (region 1) and metallic shell (region 2) placed in a solvent (region 3). This system is immersed in an homogeneous time varying electric field  $\vec{E}_0(t)$ .

where  $\vec{\Pi} = -\vec{\nabla}\psi_1$  and  $\vec{P} = -\vec{\nabla}\psi_2$ . Notice that these formulas quite similar to the previous section, except by the terms  $\vec{\Pi}$  and  $\vec{P}_2$  these are related to the polarization in the gaining material and in the metallic shell respectively. From the fact that there is no free charges in the three regions the divergence of the Displacement results Laplace equations (13) for each potential. In fact  $\Phi_{1,2,3}$  have solution as in 151617. The solutions for the remaining potentials are:

$$\psi_1 = q^1 r \cos\theta \quad (24)$$

$$\psi_2 = q^2 r + \frac{\sigma}{r^2} \cos\theta \quad (25)$$

In region 2 the polarizability is  $\vec{P}_2$  is related to the electric permittivity  $\epsilon_m = 1 + \chi_m$ . Given that this is metallic medium,  $\epsilon_m$  depends on the frequency of the impinging field, and it has a contributions due to free electrons and LSP (Equations 26 and 27):

$$\epsilon_{m,free-electrons}(\omega) = 1 - \frac{\omega_f^2}{\omega(\omega + i\gamma_f)}, \quad (26)$$

$$\epsilon_{m,lsp}(\omega) = 1 - \frac{\omega_b^2}{\omega(\omega + i\gamma_b)} \quad (27)$$

where  $\omega_f$  and  $\gamma_f$  are resonance frequency and the damping coefficient for free electrons respectively. Similarly  $\omega_b$  and  $\gamma_b$  are the resonance and the damping coefficient for bound electrons[2].

Considering now the boundary condition for the equations of the potentials(15,16,17,24,25), we may obtain the 5 following equations, a complete deduction can be found in the

literature[8]. We can numerically solve this set of equations to obtain the polarizability of the NS.

$$\frac{dq_1}{dt} + [i(\omega - \omega_{21}) + \frac{1}{\tau_2}]q_1 = \frac{iN\epsilon_h''(\omega_{21})}{2\tau_2}[E_i^* - p_3^* - (1 - \rho^3)p_2^*] \quad (28)$$

$$\frac{dN}{dt} + \frac{N - N_0}{\tau_1} = \frac{1}{\tau_1}Im\{q_1[E_i - p_3 - (1 - \rho^3)p_2]\} \quad (29)$$

$$\frac{dq_2}{dt} - \frac{i\omega}{\omega^2(1 - \epsilon_m) + 1}q_2 = -\frac{i\omega(1 - \epsilon_m)}{\omega^2(1 - \epsilon_m) + 1}[E_i - p_3 + \rho^3p_2] \quad (30)$$

$$\frac{d\sigma}{dt} - \frac{i\omega}{\omega^2(1 - \epsilon_m) + 1}\sigma = -\frac{i\omega(1 - \epsilon_m)}{\omega^2(1 - \epsilon_m) + 1}p_2 \quad (31)$$

$$p_2 = \frac{(1 - \epsilon_3)(E_i - \rho^3p_3) + q_2 - 2(q_1^* + \sigma)}{\epsilon_b + 2 - \rho^3(\epsilon_b - 1)} \quad (32)$$

$$p^3 = \frac{\frac{(1 - \epsilon_3)(\epsilon_b + 2) + \rho^3(\epsilon_b - 1)(\epsilon_3 + 2)}{(\epsilon_b + 2)(1 + 2\epsilon_3) - 2\rho^3(\epsilon_b - 1)(\epsilon_3 - 1)} E_i}{\frac{6\rho^3q_1^* + (1 - \rho^3)[(\epsilon_b + 2)q_2 - 2\rho^3(\epsilon_b - 1)\sigma]}{(\epsilon_b + 2)(1 + 2\epsilon_3) - 2\rho^3(\epsilon_b - 1)(\epsilon_3 - 1)}} \quad (33)$$

### 3 Results and discussion

In order to calculate the optical forces that would be generated in an optical trapping experiment for a NS particle, the polarizability is derived from Equations 29-33 using numerical tools. The particle considered has an external radius of 20nm and an internal radius equal to 15.4nm. The shell is made of silver whose polarizability has been extrapolated from database[9], the internal core is made of silica. The particle is immersed in ethanol. The dye molecule present in the core is Rhodamine-123, whose emission peak is around 530nm, it has to be noticed that  $\rho$  has been chosen so that the LSPR could match the peak[10]. The polarizability has been calculated by using a total of six values of gaining  $G = 0.63 \times 10^{-2} n \tau_2 \mu^2$ . The Top gain  $G = -0.22$  because we can't found steady-state solutions for higher gaining. Results in Figures 8. Notice that the Behavior of these curves are similar to the polarizability for metals as expected from the metallic shell.

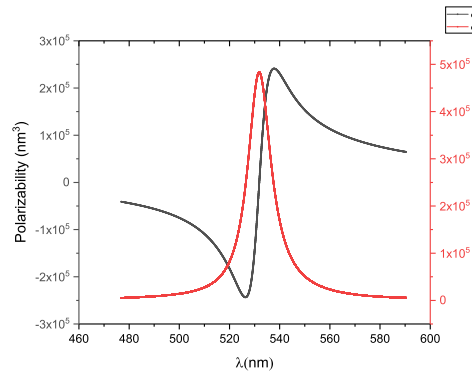


Figure 8: Nanoshell polarizability real  $Re\{\alpha\} = \alpha'$  and imaginary part  $Im\{\alpha\} = \alpha''$  as a function of the wavelength. Gaining  $G = 0$

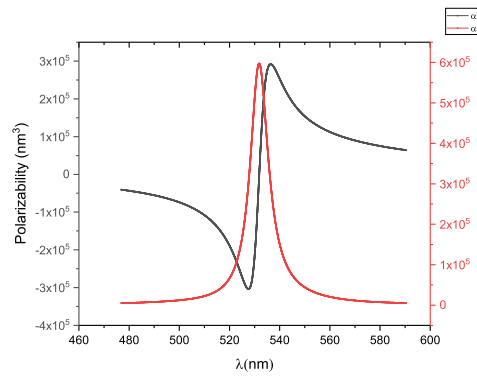


Figure 9: Nanoshell polarizability real  $Re\{\alpha\} = \alpha'$  and imaginary part  $Im\{\alpha\} = \alpha''$  as a function of the wavelength. Gaining  $G = -0.044$

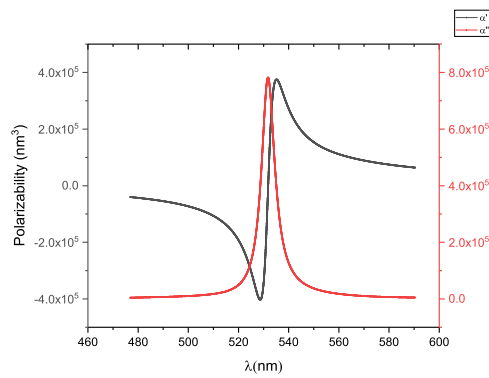


Figure 10: Nanoshell polarizability real  $Re\{\alpha\} = \alpha'$  and imaginary part  $Im\{\alpha\} = \alpha''$  as a function of the wavelength. Gaining  $G = -0.088$

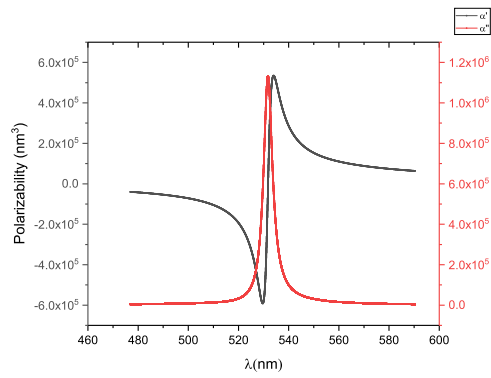


Figure 11: Nanoshell polarizability real  $Re\{\alpha\} = \alpha'$  and imaginary part  $Im\{\alpha\} = \alpha''$  as a function of the wavelength. Gaining  $G = -0.132$

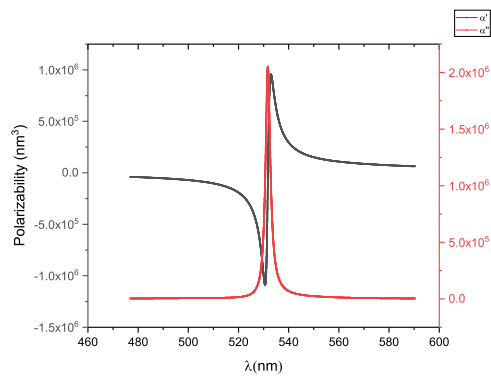


Figure 12: Nanoshell polarizability real  $Re\{\alpha\} = \alpha'$  and imaginary part  $Im\{\alpha\} = \alpha''$  as a function of the wavelength. Gaining  $G = -0.176$

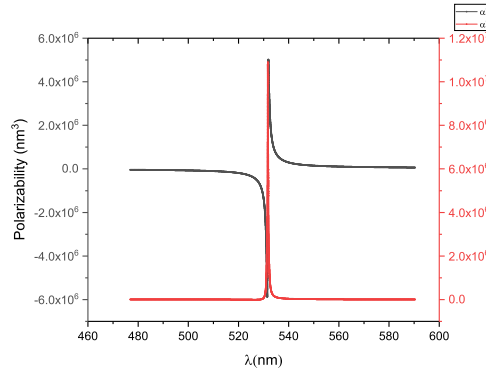


Figure 13: Nanoshell polarizability real  $Re\{\alpha\} = \alpha'$  and imaginary part  $Im\{\alpha\} = \alpha''$  as a function of the wavelength. Gaining  $G = -0.22$

### 3.1 OT counterpropagating Beams

The first OT studied consists of two counter propagating Gaussian beams (c.p.) with intensity defined by equation 34. Due to the symmetry of this system scattering forces cancel each other everywhere. The trapping constants  $k$  has been derived from equation 9, the obtained in the propagation direction (Equation 35) and in the perpendicular plane (Equation 36). Stiffness's  $\frac{k}{P}$  of the trapping are presented as a function of wavelength  $\lambda$  in figures14

$$I(\rho, z) \quad (34)$$

$$k_z^{c.p.} = 4 \frac{\alpha'}{cn_m} (2 - 2k_m z_0 + k_m^2 z_0^2) \frac{I_0}{z_0^2} \quad (35)$$

$$k_\rho^{c.p.} = 8 \frac{\alpha'}{cn_m} \frac{I_0}{\omega_0^2} \quad (36)$$

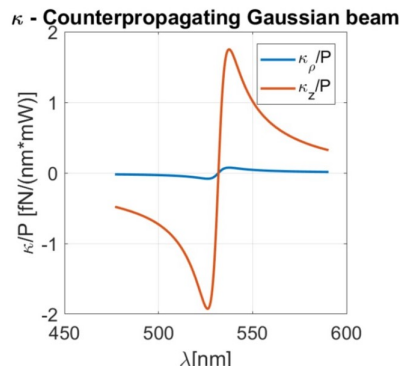


Figure 14: Stiffness ( $\frac{k}{P}$ ) of the trapping for counterpropagating gaussian beams in nanoshell particle embedding gain ( $G = 0$ ) for Parallel (in red) and perpendicular (in blue) as a function of wavelength  $\lambda$ .

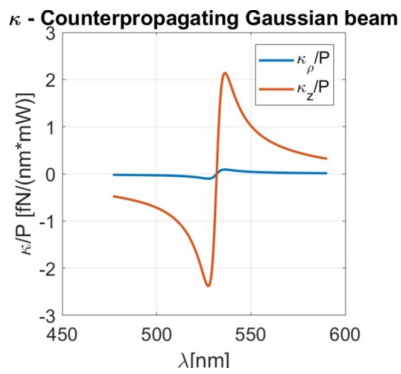


Figure 15: Stiffness ( $\frac{k}{P}$ ) of the trapping for counterpropagating gaussian beams in nanoshell particle embedding gain ( $G = -0.44$ ) for Parallel (in red) and perpendicular (in blue) as a function of wavelength  $\lambda$ .

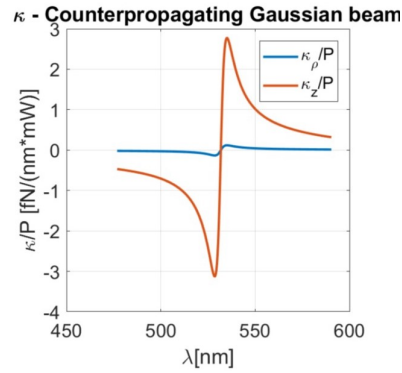


Figure 16: Stiffness ( $\frac{\kappa}{P}$ ) of the trapping for counterpropagating gaussian beams in nanoshell particle embedding gain ( $G = -0.088$ ) for Parallel (in red) and perpendicular (in blue) as a function of wavelength  $\lambda$ .

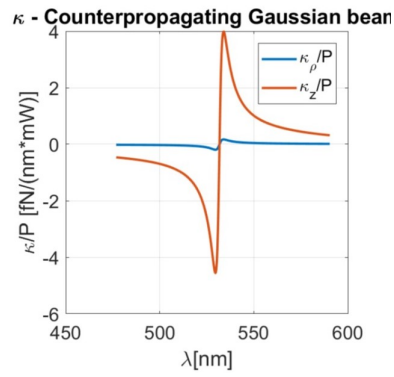


Figure 17: Stiffness ( $\frac{\kappa}{P}$ ) of the trapping for counterpropagating gaussian beams in nanoshell particle embedding gain ( $G = -0.132$ ) for Parallel (in red) and perpendicular (in blue) as a function of wavelength  $\lambda$ .

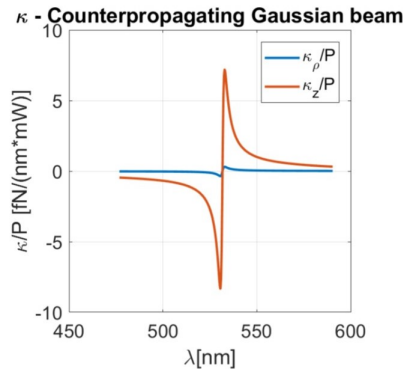


Figure 18: Stiffness ( $\frac{k}{P}$ ) of the trapping for counterpropagating gaussian beams in nanoshell particle embedding gain ( $G = -0.176$ ) for Parallel (in red) and perpendicular (in blue) as a function of wavelength  $\lambda$ .

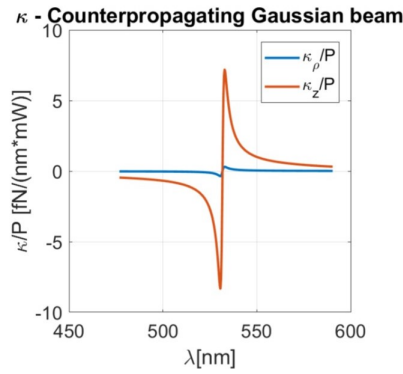


Figure 19: Stiffness ( $\frac{k}{P}$ ) of the trapping for counterpropagating gaussian beams in nanoshell particle embedding gain ( $G = -0.22$ ) for Parallel (in red) and perpendicular (in blue) as a function of wavelength  $\lambda$ .

These calculations show that for all gain values there is a range of wavelength in which the trap stiffness is negative, that as expected corresponds to the same range in which the polarizability is negative. However located on the other side of the resonance resonance there is a range of wavelength in which the trapping is possible and it corresponds to a positive polarizability. These behavior is common to all the gain levels.

Moreover, as the value of the trap stiffness increases with gain as shown in figure 3.13, we can notice by looking at figures 14-19 that the trapping range become smaller.

The gain shows a tremendous impact on the optical trapping for c.p. beams (See Figure 20) especially in the propagation direction.

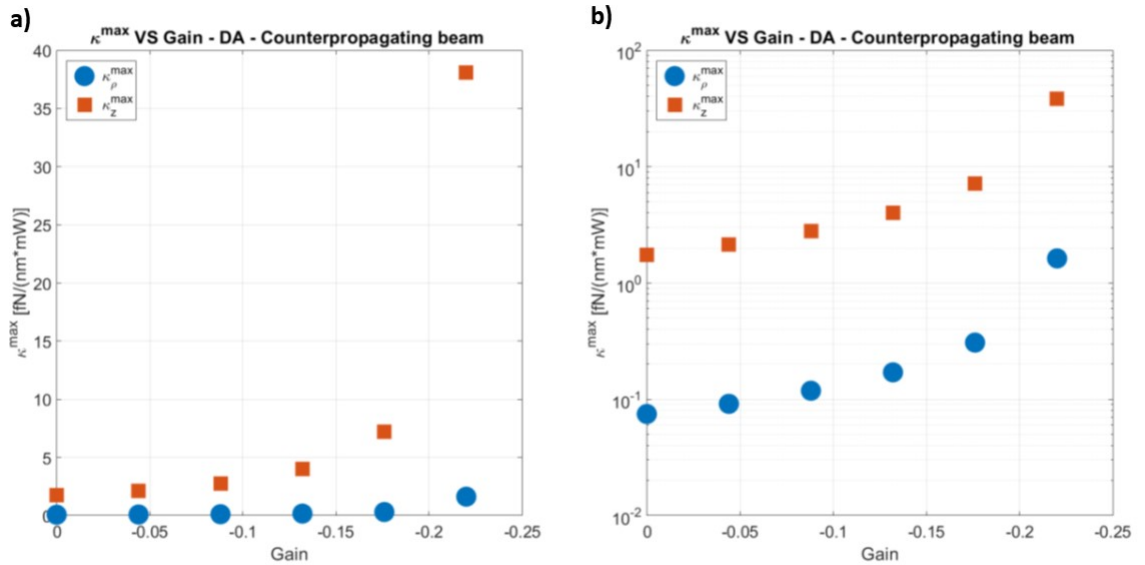


Figure 20: Maximum value for constant stiffness ( $k_P^{\max}$ ) as function of the gaining  $G$  c.p. system. In red parallel Direction, in blue perpendicular plane direction. a) Linear scaling for b) Logarithmic scaling

It's important to consider that the steady-state regime is valid until gaining of -0.22, so we cannot predict the behavior of the trap overcoming this value. After this value of gain, the system enters in the so called spaser regime, losses are completely compensated and an analogous of a laser emission is expected[11]. Achieving this regime in the experiments would bring extremely interesting and novel results. However at this border the quasi-static approximation breaks and the polarizability cannot be described as we did.

### 3.2 OT single Gaussian beam

In this section we present the calculation of optical forces for a optical trap that uses a single Gaussian beam. In this configuration the scattering force must be taken into account. Here we look at the sum of scattering and gradient force. To calculate constants  $k$  we used equations 37 and 38. Like before the stiffness of the trap at the maximum grows with gain, while the trapping region become narrower. The impact of gain on this configuration seems to be less effective. This quantities are similar to the previous ones in 14 so there is no further analysis involved. Perhaps there are presented the maximum

stiffness trapping for each gain in figure 21. Its important to notice that in these cases the trapping in the perpendicular plane is more effective that the one in the parallel direction.

$$k_z^{s.g.} = \frac{\alpha'}{cn_m} \frac{I_0}{z_0^2} \quad (37)$$

$$k_\rho^{s.g.} = 2 \frac{\alpha'}{cn_m} \frac{I_0}{\omega_0^2} \quad (38)$$

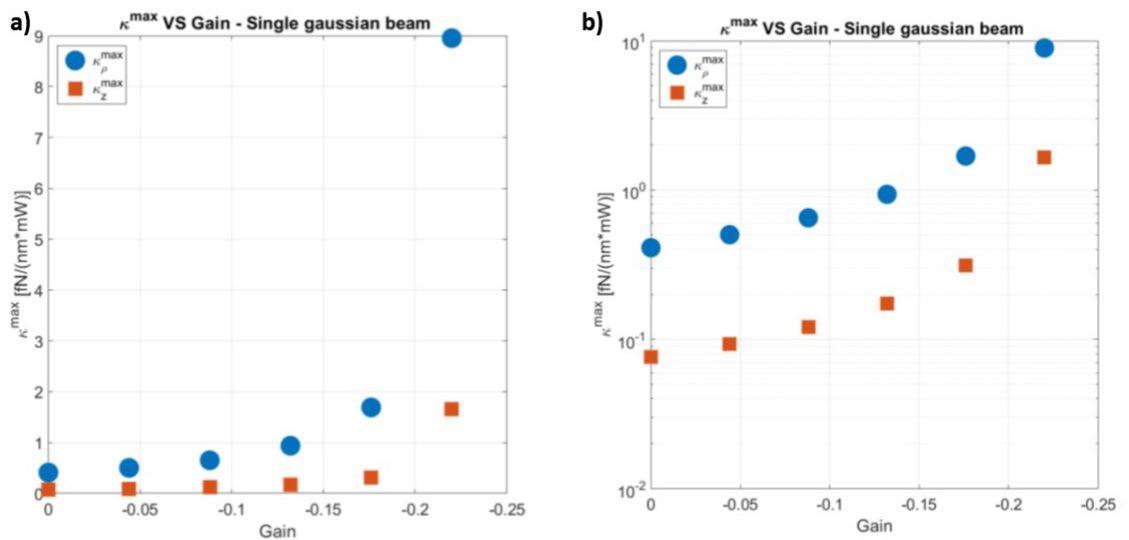


Figure 21: Maximum value for constant stiffness ( $\frac{k^{max}}{P}$ ) as function of the gaining  $G$  s.g. system. In red parallel Direction, in blue perpendicular plane direction. a) Linear scaling for b) Logarithmic scaling

In order to have an OT the summation of the forces in 9 and 11 should be negative. In figure 22 are plotted both forces as function of the wavelength, and there is also a plotted the dependence between this force and the displacement from the equilibrium position at a given  $\lambda = 590$ . We choose this wavelength because there is an optical trapping for every gain level. As shown in the figure 22 the total force is repulsive for most of the spectrum, except after a given wavelength. The main reason is that the scattering force (dependent on  $\alpha''$ ) decreases fast away from the resonance, but the gradient force (dependent on  $\alpha'$ ) decreases slower. Moreover, in the right picture the

total force is plotted as function of the displacement from the equilibrium position  $z_0$  at  $\lambda = 590.4$ . We choose this wavelength because there is optical trapping for all gaining levels. Also notice the strength of the trap in the parallel direction decrease with the gain, this is because near the resonance the complex polarizability increases faster than the real part with the level gaining.

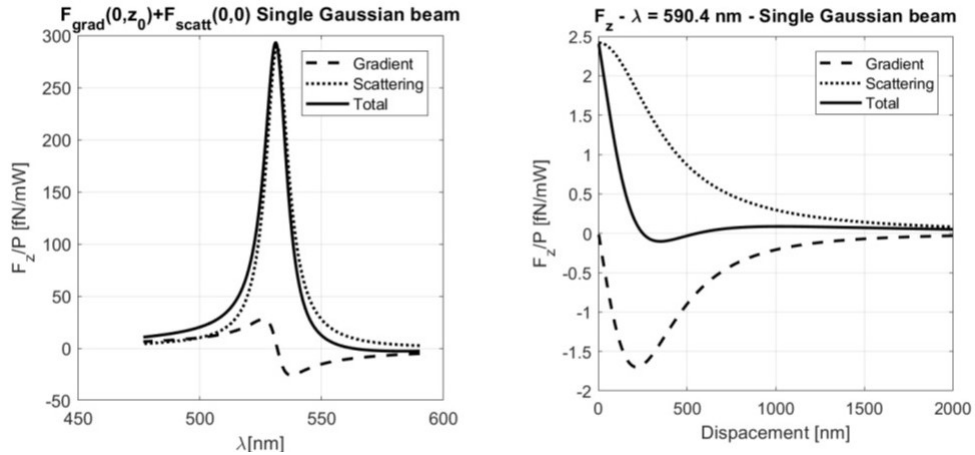


Figure 22: On the left Scattering force (dotted line), Gradient force (dashed line), and Total force (solid line) as a function of the wavelength. On the right Scattering force (dotted line), Gradient force (dashed line), and Total force (solid line) as a function of the wavelength as a function of the displacement ( $G = 0$ ).

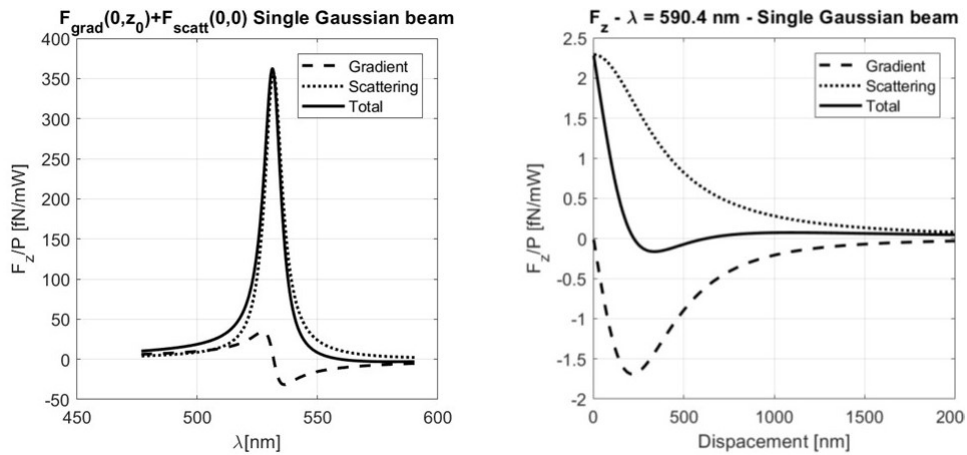


Figure 23: On the left Scattering force (dotted line), Gradient force (dashed line), and Total force (solid line) as a function of the wavelength. On the right Scattering force (dotted line), Gradient force (dashed line), and Total force (solid line) as a function of the wavelength as a function of the displacement ( $G = -0.044$ ).

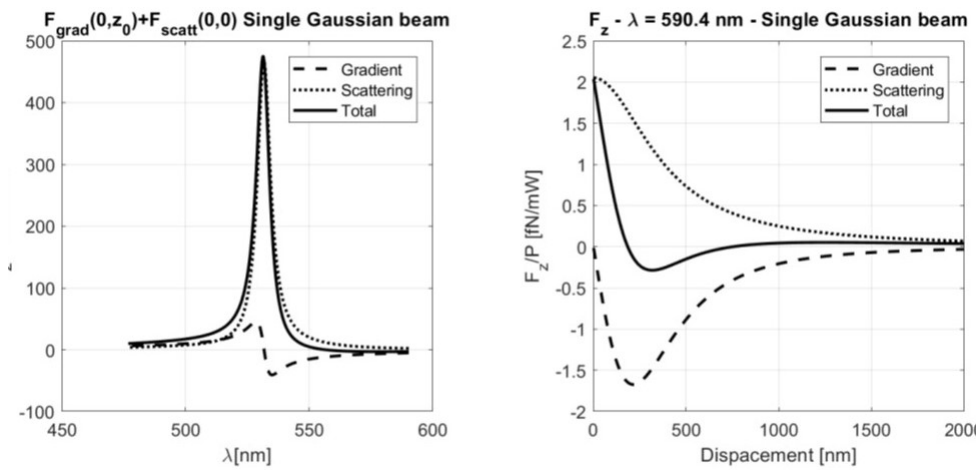


Figure 24: On the left Scattering force (dotted line), Gradient force (dashed line), and Total force (solid line) as a function of the wavelength. On the right Scattering force (dotted line), Gradient force (dashed line), and Total force (solid line) as a function of the wavelength as a function of the displacement ( $G = -0.088$ ).

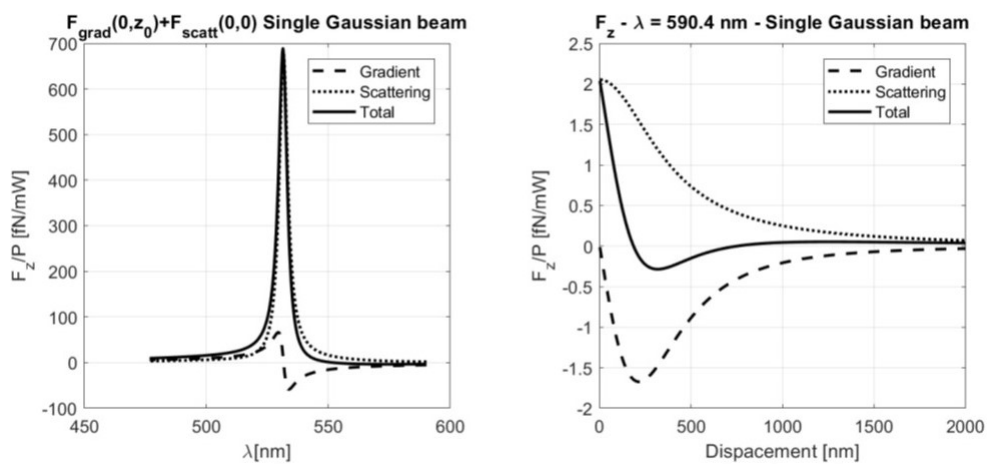


Figure 25: On the left Scattering force (dotted line), Gradient force (dashed line), and Total force (solid line) as a function of the wavelength. On the right Scattering force (dotted line), Gradient force (dashed line), and Total force (solid line) as a function of the wavelength as a function of the displacement ( $G = -0.132$ ).

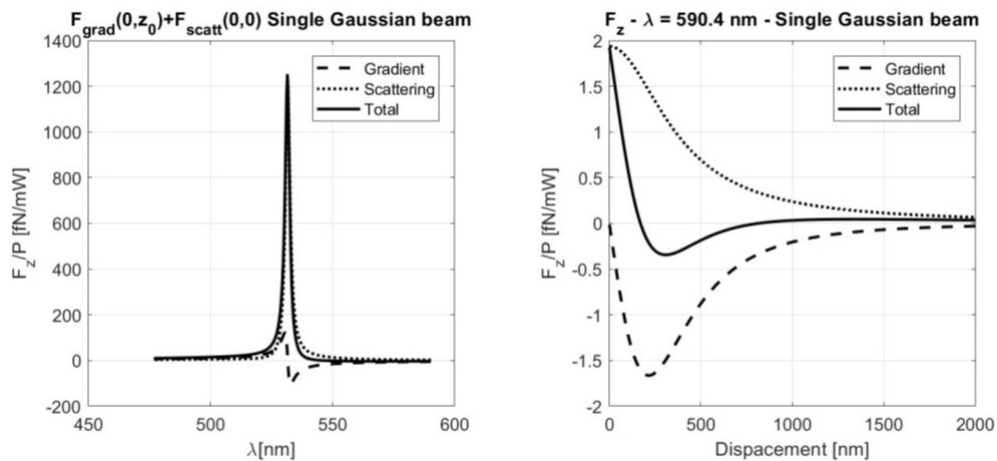


Figure 26: On the left Scattering force (dotted line), Gradient force (dashed line), and Total force (solid line) as a function of the wavelength. On the right Scattering force (dotted line), Gradient force (dashed line), and Total force (solid line) as a function of the wavelength as a function of the displacement ( $G = -0.176$ ).

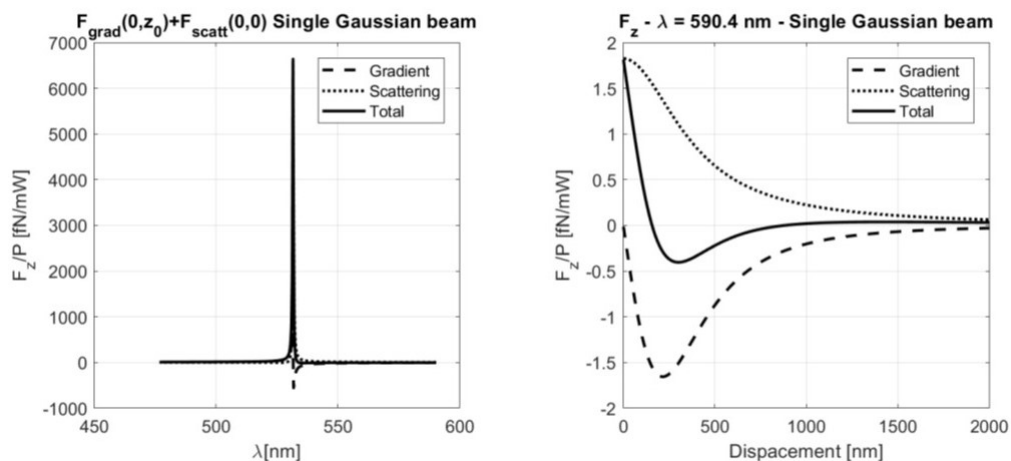


Figure 27: On the left Scattering force (dotted line), Gradient force (dashed line), and Total force (solid line) as a function of the wavelength. On the right Scattering force (dotted line), Gradient force (dashed line), and Total force (solid line) as a function of the wavelength as a function of the displacement ( $G = -0.22$ ).

## 4 Conclusions

In this work we used a quasi static approximation for the calculation of a metallic nanoshell embedding gain molecules. We used to calculate optical forces in two different experimental configuration: the single beam optical tweezers and the counter-propagating beams. The forces have been calculated for six different values of gain. The gain seems to affect the optical force in particular the trap stiffness grows with the gain level, more importantly for the c.p. than for a single beam OT. However the trapping spectral region is becoming narrower with gain. These calculations are a good indication for experiments. Optical tweezers experiment are a good tool to prove plasmon gain coupling and could represent an important tool to distinguish between the steady-state and the emission regime.

## 5 References

### References

- [1] Ashkin, A. (1970, Jan). Acceleration and trapping of particles by radiation pressure. *Phys. Rev. Lett.*, 24, 156–159. Retrieved from <https://link.aps.org/doi/10.1103/PhysRevLett.24.156> doi: 10.1103/PhysRevLett.24.156
- [2] Jones, P. H., Maragó, O. M., & Volpe, G. (2015). *Optical tweezers: Principles and applications*. Cambridge University Press.
- [3] Maier, S. A. (2007). *Plasmonics: fundamentals and applications*. Springer Science & Business Media.
- [4] Hirsch, L. R., Stafford, R. J., Bankson, J., Sershen, S. R., Rivera, B., Price, R., . . . West, J. L. (2003). Nanoshell-mediated near-infrared thermal therapy of tumors under magnetic resonance guidance. *Proceedings of the National Academy of Sciences*, 100(23), 13549–13554.
- [5] Veltri, A., Chipouline, A., & Aradian, A. (2016). Multipolar, time-dynamical model for the loss compensation and lasing of a spherical plasmonic nanoparticle spaser immersed in an active gain medium. *Scientific reports*, 6, 33018.
- [6] Zhang, H., Zhou, J., Zou, W., & He, M. (2012). Surface plasmon amplification characteristics of an active three-layer nanoshell-based spaser. *Journal of Applied Physics*, 112(7), 074309.
- [7] Halas, N. (2005). Playing with plasmons: tuning the optical resonant properties of metallic nanoshells. *Mrs Bulletin*, 30(5), 362–367.
- [8] Cathey, A. (2016). *Spaser Instability in Gain-Assisted Silver Nanoshell* (Undergraduate thesis). Universidad San Francisco de Quito USFQ: Quito.
- [9] Johnson, P. B., & Christy, R.-W. (1972). Optical constants of the noble metals. *Physical review B*, 6(12), 4370.
- [10] Dixon, J. M., Taniguchi, M., & Lindsey, J. S. (2005). PhotochemCAD 2: A Refined Program with Accompanying Spectral Databases for Photochemical Calculations. *Photochemistry and photobiology*, 81(1), 212-213.
- [11] Bergman, D. J., & Stockman, M. I. (2003). Surface plasmon amplification by stimulated emission of radiation: quantum generation of coherent surface plasmons in nanosystems. *Phys. Rev. Lett.*, 90(2), 027402.